# Defect-induced room temperature ferromagnetic properties of the Al-doped and undoped ZnO rod-like nanostructure

**Article** *in* Materials Letters · April 2017
DOI: 10.1016/j.matlet.2017.04.064



**5 authors**, including:

Leta Jule
Adama Science and Technology University
**7** PUBLICATIONS **19** CITATIONS
SEE PROFILE

F. B. Dejene
University of the Free State
**187** PUBLICATIONS **742** CITATIONS
SEE PROFILE

Abdub G. Ali
Meru University College of Science and Technology
**4** PUBLICATIONS **11** CITATIONS
SEE PROFILE

Kittessa Roro
Council for Scientific and Industrial Research, South Africa
**32** PUBLICATIONS **238** CITATIONS
SEE PROFILE

Materials Letters 199 (2017) 151–155

Contents lists available at ScienceDirect

Materials Letters

journal homepage: www.elsevier.com/locate/mlblue

# Defect-induced room temperature ferromagnetic properties of the Al-doped and undoped ZnO rod-like nanostructure

Leta Jule [a,*], Francis Dejene [a], Abdub G. Ali [a], Kittessa Roro [b], Bonex Mwakikunga [c]

[a] Physics Department, University of the Free State, Private Bag X13, Phuthaditjhaba 9866, South Africa
[b] CSIR-Energy center, Council for Scientific and Industrial Research, P.O. Box 395, Pretoria, South Africa
[c] CSIR- National Centre for Nano-Structured Materials, P.O. Box 395, Pretoria 0001, South Africa

ARTICLE INFO

*Article history:*
Received 10 February 2017
Received in revised form 6 April 2017
Accepted 12 April 2017
Available online 17 April 2017

*Keywords:*
Sol-gel preparation
Magnetic materials
EPR
Ferromagnetism
ZnO

ABSTRACT

In this work, electron paramagnetic resonance (EPR) experiment on undoped ZnO and Al doped ZnO (AZO) nanoparticles prepared by facile sol–gel method were investigated. The effects of the Al concentration on room temperature ferromagnetic (FM) properties of the AZO ($Zn_{1-x}Al_xO, 0.1 \leqslant x \leqslant 0.30$) are reported. EPR signal reveals the origin of FM is purely intrinsic and related with interaction of clusters carrying net magnetic moment coming from electron spin trapped in defect states. Increasing Al concentration results in reducing FM ordering which are likely due to reduction in amount of oxygen adsorption. Defect analysis based on PL, indicates zinc interstitials ($Zn_i$) and singly oxygen vacancies ($Vo^+$) are responsible for mediating ferromagnetism in the undoped ZnO. The assertion was supported by Raman spectra and EPR analysis. Moreover, the present work suggests the potential applications of AZO in future spintronics and speculate the origin of ferromagnetism in AZO nanoparticles.



## 1. Introduction

ZnO with a direct band gap of 3.3–3.4 eV attracts considerable attention due to its applications like UV light emitters, varistors, transparent high power electronics, surface acoustic wave devices, piezoelectric transducers, gas sensing and as window material for display and solar cells [1,2]. Doped ZnO nanocrystals, which can be easily processed at temperatures much lower than those for bulk ZnO crystals, are of particular interest because of their potential for use in light-emitting devices. Doping semiconductor with foreign elements to manipulate their electrical and magnetic properties is an important aspect for the realization of various types of advanced nanodevices [3].

After the theoretical prediction of room temperature ferromagnetism (RTFM) in Mn-doped ZnO by Dietl et al. [4], ZnO doped with magnetic transition metal (TM) ions was intensively studied due to its potential applications in future spintronic devices, magneto-optics and magnetoelectronics [1]. Sergei et al. [5] reported the identification of Li and Na as interstitial shallow donors in ZnO nanocrystals, however the device application is not practical because of the challenge in controlling the concentration of donor impurities. The high frequency EPR analysis done by Pavel et al. [6] indicates the preference of Al, Ga or In as substitutional impurities as they form shallow donors in single crystals of ZnO by replacing Zn atoms.

Al is among the dopant that can be used to enhance phonon scattering, improve the electrical conductivity and can replace traditional tin-doped indium oxide(ITO) transparent conducting oxide (TCO) films, which are essential components for a large variety of optoelectronic devices, acting as transparent electrical contacts or electrodes [7–9]. Reviews by Klingshirn et al. [10] on ZnO proposed the substitution of $Zn^{2+}$ ions by $Al^{3+}$ ions may induce more point defects for the different ionic radii of $Al^{3+}$ and $Zn^{2+}$ ions. Indeed, the assertion was proved by Gao et al. [11] on their ferromagnetic study of ZnO nanoparticles doped with nonmagnetic element, Al. If this is the case, according to the $d^0$ ferromagnetism, proposed by Zhang et al. [12] it is expected that the room temperature ferromagnetism (RTFM) can be achieved in Al-doped ZnO without Al metal clusters or the interfaces of Zn and Al. Recent studies by Ma et al. [13] group also suggests the induced RTFM in the Al/ZnO film is due to the interaction of metal clusters and the ZnO matrix. The observation by Chen et al. [14] also confirms the origin of RTFM in Al doped ZnO is likely due to the charge transfer between Zn and Al at the interfaces of nanograins.

However, in the present study the role of zinc interstitials and singly ionized oxygen vacancies as the origin of RTFM in undoped

* Corresponding author.
*E-mail address:* leta.2010@yahoo.com (L. Jule).

http://dx.doi.org/10.1016/j.matlet.2017.04.064
0167-577X/

ZnO are discussed. Moreover the various concentration of Al on FM ordering of AZO nanoparticles using EPR signal are investigated.

## 2. Experimental

ZnO and AZO nanoparticles were synthesized by sol–gel method reported elsewhere [15,16]. The precursor used to prepare the sol are Zinc acetate dehydrate $[Zn(CH_3COO)_2.2H_2O]$ which was dissolved into 2-methoxyethanol $[C_3H_80_2]$ as a solvent and monoethanolamine are used to stabilize the solution. To prepare AZO aluminum nitrate nonahydrate $Al(NO_3)_3.9H_2O$ were used as aluminium source for the prepared samples. In the process the doped concentration of Al/Zn = 0.1, 0.15, 0.2, 0.25, 0.3 were prepared. The structure of the samples were characterized by X-ray diffractometry (XRD) with Cu K $\alpha$ (1.5418Å) radiation and the surface morphology of the nanoparticles are investigated by scanning electronic microscopy (SEM) ZU SSX-550. The ferromagnetic properties was studied using JEOL x-band electron paramagnetic resonance (EPR) which operates at frequency of 9.4 GHz. The samples were set to be placed at the center of the cavity where magnetic field of the microwave is maximum. However, the power was kept at 5 mW and the $H_{DC}$ field was slowly varied in between 0 and 500 mT. Finally, the response was measured as a derivative of microwave absorption signal. Perkin Elmer UV/Vis and (PL) (He-Cd) laser system 5.0 with an excitation 248.6 nm are used to measure the luminescence of the samples.

## 3. Results and discussion

The phases and structures of the samples are identified using XRD spectra. Fig. 1 A shows XRD patterns of undoped ZnO and Al doped ZnO which were indexed as a polycrystalline hexagonal wurtzite structure of ZnO. The crystallographic direction are labelled according to (JCPDS card No. 36 – 1451). The spectra shows there are no formation of secondary phase observed in the samples. The strong peak along (101) from the spectra suggest the preferred crystal orientation. The calculated lattice parameter and the shift in peak towards the larger angle are displayed in Table 1. Fig. 1B shows $\omega_{scan}$ (rocking curve) for the samples indicating the shifts towards the higher angles which is indicative of a compressive stress incorporated in the ZnO lattice.

Fig. 2 shows the morphology and the elemental composition of the samples taken using scanning electron microscopy (SEM). Fig. 2,A, B, C, D and E shows the SEM micrograph of the samples with undoped ZnO, $x = 0.1, x = 0.15, x = 0.20$ and $x = 0.30$ respectively. The EDX spectras of the samples with $x = 0.0$, $x = 0.1, x = 0.15, x = 0.2, x = 0.25$ and $x = 0.3$ are shown in Fig. 2, F, G, H, I, J and K. The micrographs exhibited the formation of rod-like structures having diameters almost ranging from 0.6 to 1 μm. The packed rods become more visible as Al content increases which might be indicative of Al doping would result in ZnO grains growing preferentially with c-axis parallel to the ZnO host crystal. However, the intensity of the XRD peak (002) which is related to c-axis doesn't change with Al doping this is likely because of the intrinsic stress induced in the host matrix which can be supported by the rocking curve in Fig. 1B. In addition the variation in ionic radii of $Al^{3+}$ compared to $Zn^{2+}$ might be the reason for the observed SEM transformation. The EDX pattern also confirms the existence of all expected elemental compositions (Zn, O and Al) and the possibility of induced point defects formation coming from Zinc interstitial and oxygen vacancy.

To characterize the paramagnetic defects or centers in the samples EPR spectroscopy were used. The techniques are effective in identifying unpaired electrons so that surface defects, radicals, cations or clusters are easily detected through EPR signals. Therefore, EPR measurements are taken with microwaves having power with 5 mW by fixing the frequency at 9.4 GHz. By increasing DC field from 1 mT to 6 mT at 100 kHz, the difference in energy between the two states is widened until it matches the energy of the microwaves. Fig. 3A shows the microwave response as a function of magnetic flux density (DC field) for undoped ZnO and Al doped ZnO samples at room temperature. As indicated there are two absorption peaks at 150 and 300 mT which are ascribed to paramagnetism and ferromagnetism resonant field, respectively. The former will be due to magnetic clusters situated near the surface which are emanated from electron spin trapped in the defects. As indicated in Fig. 3B around 300 mT and 350 mT field there are hyperfine line coupling which become broader with increase in Al concentration due to exchange interaction of dopant ions. Although the exact mechanism of intrinsic FM in undoped oxides is still under debate, defects have greatly been suggested to play

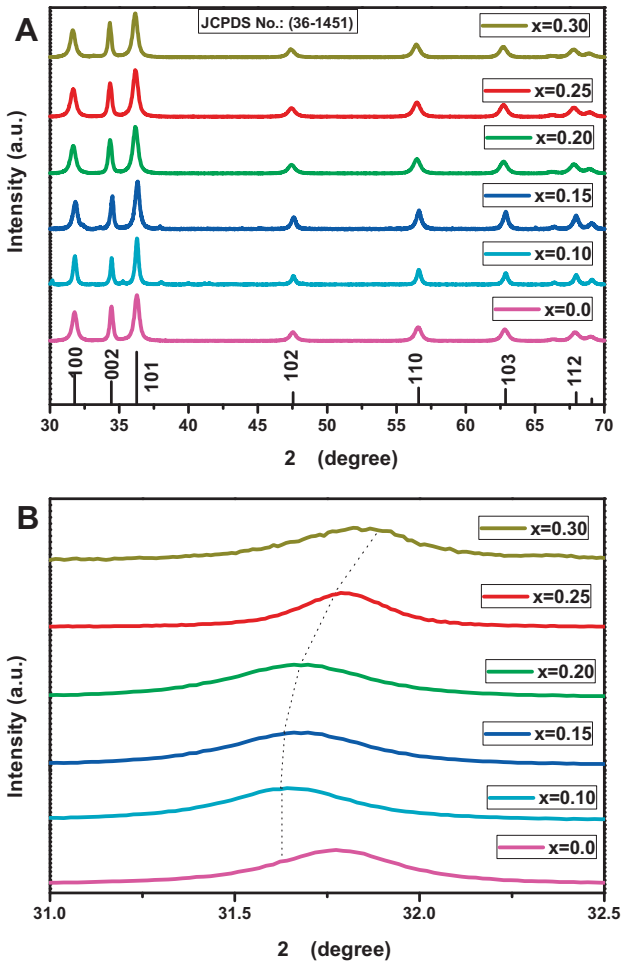


**Fig. 1.** A.XRD patterns of undoped and Al doped ZnO nanocrystalline powders for different Al concentrations B. $\omega_{scan}$(rocking curve) for samples having Al concentration at x = 0.15, x = 0.20, x = 0.25, x = 0.30.

**Table 1**
The calculated lattice constants of Al doped and undoped ZnO.

| Al Concent. | $2\theta$ | Lattice constants, a (Å) | Lattice constants, c (Å) |
|---|---|---|---|
| 0.00% | 31.77 | 3.248 | 5.299 |
| 0.10% | 31.64 | 3.247 | 5.302 |
| 0.15% | 31.65 | 3.245 | 5.305 |
| 0.20% | 31.69 | 3.243 | 5.307 |
| 0.25% | 31.77 | 3.241 | 5.307 |
| 0.30% | 31.91 | 3.240 | 5.307 |

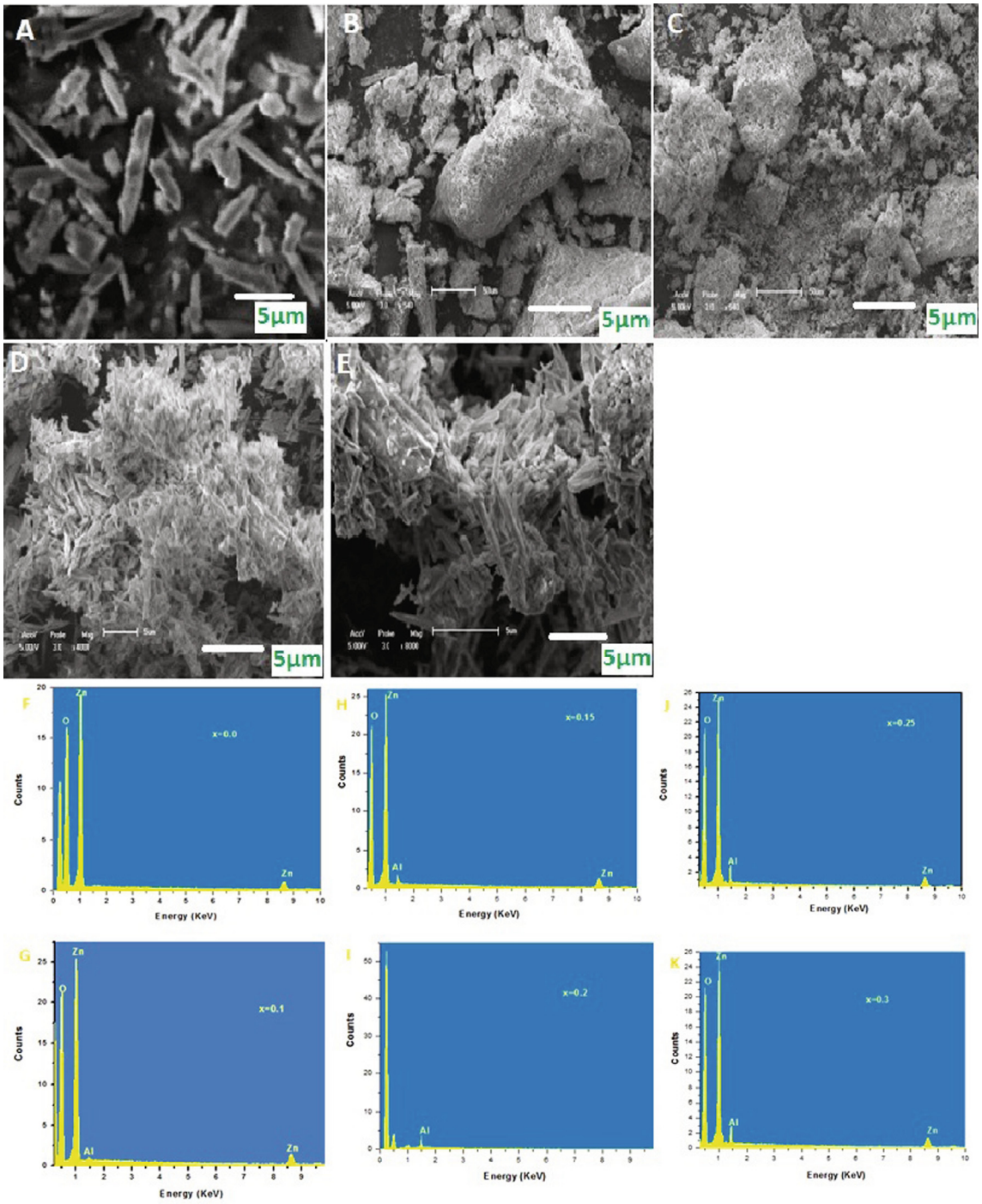


**Fig. 2.** SEM micrograph and EDX spectrum of ZnO nanoparticles at: (A) undoped ZnO. (B)$x = 0.1$. (C)$x = 0.15$ (D)$x = 0.20$ (E)$x = 0.30$ and F, G, H, I, J and K are the corresponding EDX spectras of $x = 0.0, x = 0.1, x = 0.15, x = 0.20, x = 0.25$ and $x = 0.3$, respectively.

an important role in the FM origin in the undoped ZnO system [17]. However, in the present work we suggest that the origin of FM in undoped ZnO comes from the intrinsic exchange interaction of magnetic moments in the sample. The PL analysis, which predicts the existence of single oxygen vacancies carrying a net magnetic moment underscore the assertion to the origin of FM are defect induced. However, the role of defects in mediating the FM in undoped ZnO still needs further theoretical and experimental studies.

Room temperature photoluminescence (PL) spectra of ZnO for Al doped and undoped ZnO has been investigated. Fig. 4 shows room temperature PL spectrum with various Al concentration. Here, in the spectra, three emission peaks at around 450, 500 and 520 nm are observed. The blue emission at around 450 nm is assigned to electronic transitions from Zn interstitial levels ($Z_{ni}$) to valence band where as the green emission at around 500 nm is ascribed to singly ionized oxygen vacancies ($V_o^+$) [1,18–20]. The emission at 520 nm is likely due to the doubly ionized oxygen vacancy ($V_o^{++}$). Moreover, in the present work these defects are suggested as the origin of room temperature FM observed in un-doped ZnO structures.

Raman scattering measurements were recorded to study the vibration modes in the un-doped ZnO and Al doped ZnO structures, as shown in Fig. 5. The Raman spectrum of the un-doped ZnO

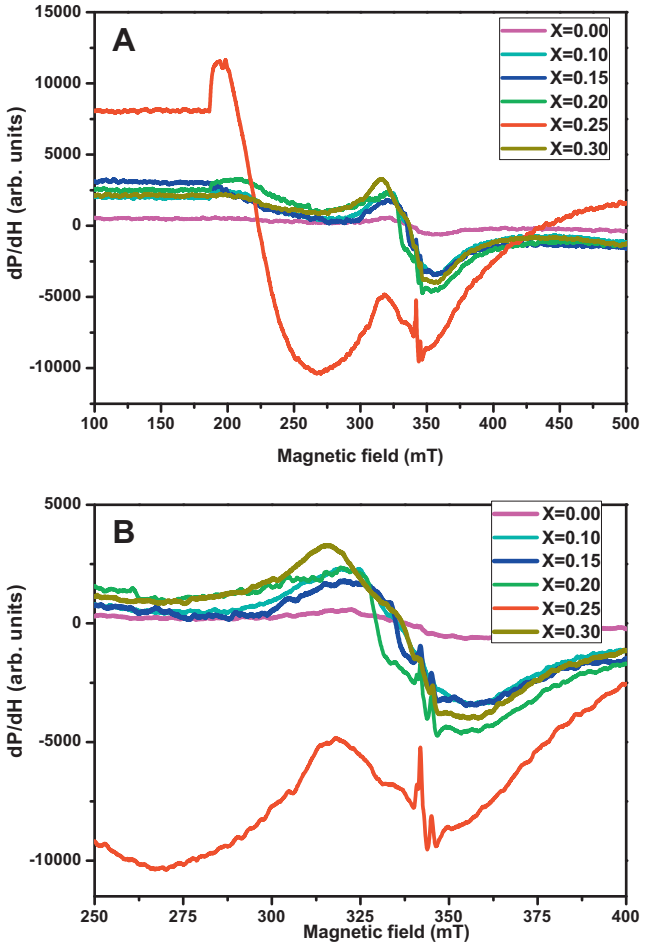


**Fig. 3.** A. EPR measurements for the undoped and Al doped ZnO. B. Shows the enlarged EPR measurements.

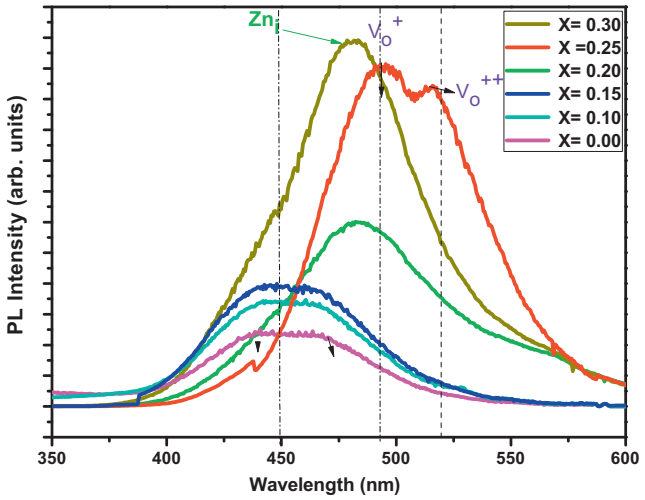


**Fig. 4.** PL emission of ZnO nanoparticles synthesized at various concentration of Al doped ZnO and undoped ZnO.

nanostructures shows the conventional vibration modes of $A_1(TO)$ and $E_{2H}$ at around, $380cm^{-1}$ and $438cm^{-1}$ [17], which have correlation with oxygen vacancies [21–23]. The peak position of the $E_2(high)$ mode, which is related to the oxide ion vibration, shifts toward a lower frequency as the oxygen vacancies increase, which

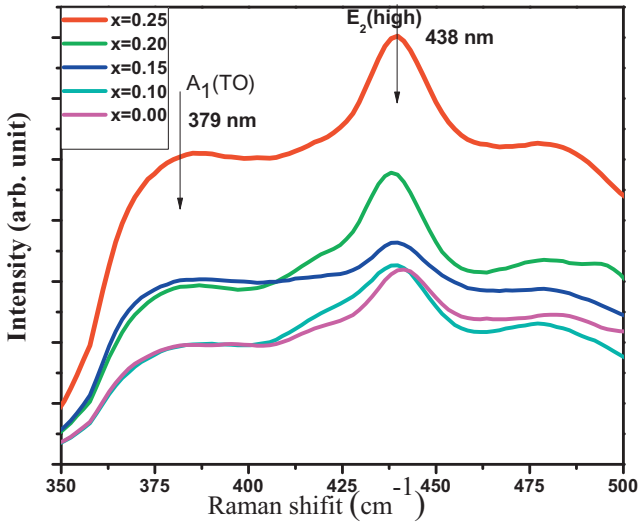


**Fig. 5.** Raman spectra of undoped ZnO and Al doped Zinc Oxide for different concentration of Al.

helps to scale the amount of oxygen vacancies as similar conclusion are drawn by Fukushima et al. [24]. Despite the fact that oxygen vacancies related scattering in all samples are very small from Raman spectra, the room temperature PL shows existence of oxygen related defects in the samples. However, the increase in intensity of Raman peaks with increase in Al concentration might be related with band shift and distortion of FM ordering.

## 4. Conclusions

We have successfully synthesized undoped ZnO and Al doped ZnO nanostructures by facile sol–gel approach. The effects of Al concentration on the magnetic, optical and structural morphology are investigated. EPR clearly indicates the hyperfine splitting in the samples, and in addition it confirms defects, in particular, zinc interstitials and singly ionized oxygen vacancies, are the origin of ferromagnetism in undoped ZnO nanostructure. However, in the Al-doped ZnO nanostructure, the suppression of FM ordering might be ascribed to the formation of Al short range orders. The structural analysis performed by SEM images, XRD, and EDX spectra reveals that the prepared samples possess hexagonal wurzite polycrystalline structures. In addition, the PL spectra indicates the presence of defects in the synthesized samples and also successfully incorporation of $Al^{3+}$ into the ZnO lattice. The analysis of Raman spectra also confirms this assertions.

## Acknowledgements

This work was supported financially by department of Physics University of the Free State research directorate.

## References

[1] Y.U. Ozgur, Y.I. Alivov, C. Liu, A. Teke, M.A. Reshchikov, S. DoÄŸan, V. Avrutin, S.-J. Cho, H. MorkoÃş, J. Appl. Phys. 98 (4) (2005) 041301, http://dx.doi.org/10.1063/1.1992666.
[2] Z. Zang, A. Nakamura, J. Temmyo, Opt. Express 21 (9) (2013) 11448–11456, http://dx.doi.org/10.1364/OE.21.011448.
[3] J. Du, M. Wang, X. Tang, Z. Zang, X. Zeng, Opt. Lett. 41 (15) (2016) 3463–3466, http://dx.doi.org/10.1364/OL.41.003463.
[4] T. Dietl, H. Ohno, F. Matsukura, J. Cibert, D. Ferrand, Science 287 (5455) (2000) 1019–1022, http://dx.doi.org/10.1126/science.287.5455.1019.
[5] S.B. Orlinskii, J. Schmidt, P.G. Baranov, V. Lorrmann, I. Riedel, D. Rauh, V. Dyakonov, Phys. Rev. B 77 (2008) 115334, http://dx.doi.org/10.1103/PhysRevB.77.115334.

[6] Celso de Mello Donegá, Jan Schmidt, Pavel G. Baranov, Sergei B. Orlinskii, Appl. Magn. Reson. 39 (10) (2010) 151–183, http://dx.doi.org/10.1007/s00723-010-0151-y.
[7] W. Liu, W. Li, Z. Hu, Z. Tang, X. Tang, J. Appl. Phys. 110 (1) (2011) 013901, http://dx.doi.org/10.1063/1.3601107.
[8] S.F.Y.J.S.C.T.S. Herng, S.P. Lau, K.S. Teng, J. Magn. Magn. Mater. 320 (2008) 107–112, http://dx.doi.org/10.1016/j.jmmm.2007.05.012.
[9] A.P. Thurber, G.L. Beausole II, G.A. Alanko, J.J. Anghel, M.S. Jones, L.M. Johnson, J. Zhang, C.B. Hanna, D.A. Tenne, A. Punnoose, J. Appl. Phy. 109 (7) (2011), 07C305.
[10] C. Klingshirn, Phys. Status Solidi (B) 244 (9) (2007) 3027–3073, http://dx.doi.org/10.1002/pssb.200743072.
[11] D. Gao, J. Zhang, G. Yang, J. Zhang, Z. Shi, J. Qi, Z. Zhang, D. Xue, J. Phys. Chem. C 114 (32) (2010) 13477–13481, http://dx.doi.org/10.1021/jp103458s.
[12] Z. Zhang, U. Schwingenschlogl, I.S. Roqan, RSC Adv. 4 (2014) 50759–50764, http://dx.doi.org/10.1039/C4RA06237J.
[13] Y.W. Ma, J.B. Yi, J. Ding, L.H. Van, H.T. Zhang, C.M. Ng, Appl. Phys. Lett. 93 (4) (2008) 042514, http://dx.doi.org/10.1063/1.2966360.
[14] S.J. Chen, K. Suzuki, J.S. Garitaonandia, Appl. Phys. Lett. 95 (17) (2009) 172507, http://dx.doi.org/10.1063/1.3254224.
[15] X. Yu, X. Yu, J. Zhang, H. Pan, Mater. Lett. 161 (2015) 624–627, http://dx.doi.org/10.1016/j.matlet.2015.09.017.
[16] L.T. Jule, F.B. Dejene, A.G. Ali, K.T. Roro, A. Hegazy, N.K. Allam, E.E. Shenawy, J. Alloy. Compd. 687 (2016) 920–926, http://dx.doi.org/10.1016/j.jallcom.2016.06.176.
[17] D.E. Motaung, I. Kortidis, D. Papadaki, S.S. Nkosi, G.H. Mhlongo, J. Wesley-Smith, G.F. Malgas, B.W. Mwakikunga, E. Coetsee, H.C. Swart, G. Kiriakidis, S.S. Ray, Appl. Surface Sci. 311 (2014) 14–26, http://dx.doi.org/10.1016/j.apsusc.2014.04.183.
[18] K. Chen, T. Fang, F. Hung, L. Ji, S. Chang, S. Young, Y. Hsiao, Appl. Surf. Sci. 254 (18) (2008) 5791–5795, http://dx.doi.org/10.1016/j.apsusc.2008.03.080.
[19] Yajun Wang, Hao Shen, Wangchang Geng, Fuli Zhang, Libing Duan, Xiaoru Zhao, J. Alloy. Compd. 645 (2015) 529–534, http://dx.doi.org/10.1016/j.jallcom.2015.05.084.
[20] J. Wang, S. Hou, H. Chen, L. Xiang, J. Phys. Chem. C 118 (33) (2014) 19469–19476, http://dx.doi.org/10.1021/jp5058226.
[21] X.J. Liu, Fei Zeng, F. Pan, C. Song, Mater. Sci. Eng.: R: Rep. 62 (1) (2008) 1–35, http://dx.doi.org/10.1016/j.mser.2008.04.002.
[22] Yage Zang, Libing Duan, Xiaoru Zhao, Mater. Lett. 162 (2016) 199–202, http://dx.doi.org/10.1016/j.matlet.2015.10.023.
[23] Lars Jeurgens, Zumin Wang, Fritz Phillipp, Yu-Chun Chen, Eberhard Goering, Appl. Phys. Lett. 103 (16) (2013) 162405, http://dx.doi.org/10.1063/1.4825268.
[24] H. Fukushima, T. Kozu, H. Shima, H. Funakubo, H. Uchida, T. Katoda, K. Nishida, in: 2015 Joint IEEE International Symposium on the Applications of Ferroelectric (ISAF), 2015, pp. 28–31.